Available online at www.sciencedirect.com
ScienceDirect
Journal of the European Ceramic Society 28 (2008) 371–376
www.elsevier.com/locate/jeurceramsoc

Observation of dislocation assisted high temperature deformation in mullite and mullite composites

Lili Taherabadi, Joy E. Trujillo, Tiandan Chen, John R. Porter, Martha L. Mecartney *

University of California, Irvine, Department of Chemical Engineering and Materials Science, Irvine, CA 92697-2575, United States

Available online 22 May 2007

Abstract

Fine grain alumina–mullite–zirconia composites demonstrate high strain rate superplastic flow ($10^{-2}\,s^{-1}$) under compression at 1400–1500 °C. Transmission electron microscopy (TEM) studies reveal dislocation activity in mullite grains of the deformed material, indicating that dislocations are generated and propagated during deformation as an accommodation mechanism for superplastic deformation. To further study dislocation accommodated slip in mullite, polycrystalline mullite in ratios of $3Al_2O_3{\cdot}2SiO_2$ and $2Al_2O_3{\cdot}1SiO_2$ were fabricated by reactive sintering of nanocrystalline alumina and colloidal silica. The strain rate of the resultant mullite was four orders of magnitude lower than the alumina–mullite–zirconia composite material. Dislocation generation accommodated the deformation of nominally single-phase polycrystalline mullite compositions at 1450 °C under 40 MPa. Three types of dislocations were observed, with a few dislocations having the character **b** = [0 0 1]. Dislocation accommodated deformation at high temperatures is significant in mullite and the complex structure of mullite may activate multiple slip systems at high temperatures.

Keywords: Creep; Mullite; Dislocations

1. Background

Superplastic ceramics have the ability to deform over 100% without fracture at high temperatures. Ceramics that have demonstrated superplasticity include single phase systems such as yttria stabilized tetragonal zirconia polycrystals (Y-TZP),[1] two phase systems such as zirconia–mullite,[2] Y-TZP with silica[3] and, yttria cubic stabilized zirconia (Y-CSZ) with silica additions.[4] More recently, three phase systems such as alumina–spinel–TZP[5] and alumina–mullite ($3Al_2O_3{\cdot}2SiO_2$)–TZP[6] have shown high strain rate potential. The key to superplastic deformation in all of these systems is the fabrication of a material with a fine grain size (usually less than 1 μm for ceramics) and limited grain growth upon high temperature deformation.[7]

Applications of superplastic forming require a high strain rate to make the process commercially feasible, thus achieving as high a strain rate as possible is one goal of superplastic research. An empirical equation that links the strain rate ($\delta\varepsilon/\delta t$) that can be achieved with the applied stress (σ), grain size (d), and temperature (T) is given in Eq. (1), where A is a material constant, n the stress exponent (usually 1–3), Q the activation energy, and R is the gas constant. It can be seen that the strain rate is inversely proportional to the grain size d, to the power of the grain size exponent p (usually 2 or 3):

$$\dot{\varepsilon} = A\frac{\sigma^n}{d^p}\exp\left(\frac{-Q}{RT}\right) \tag{1}$$

Superplastic deformation has some other unique characteristics, which differentiate it from high temperature creep. In superplastic deformation, the grains remain the same shape, and do not elongate, as would be observed in Coble creep. Deformation occurs primarily by grain boundary sliding in superplastic deformation. Yet some accommodation for grain boundary sliding is required, either the formation of cavities (which would lead to premature failure), grain boundary migration, diffusional accommodation, liquid/viscous phase accommodation, or dislocation generation.[8] It has been generally accepted that most ceramic superplastic systems that are primarily single phase have diffusional accommodation.

Diffusional accommodation, however, is difficult in three-phase ceramics. These materials maintain their fine grain size due to limited grain growth as a result of the microstructure,

* Corresponding author. Tel.: +1 949 824 2919; fax: +1 949 824 2541.
E-mail address: martham@uci.edu (M.L. Mecartney).

0955-2219/$ – see front matter © 2007 Elsevier Ltd. All rights reserved.
doi:10.1016/j.jeurceramsoc.2007.03.005

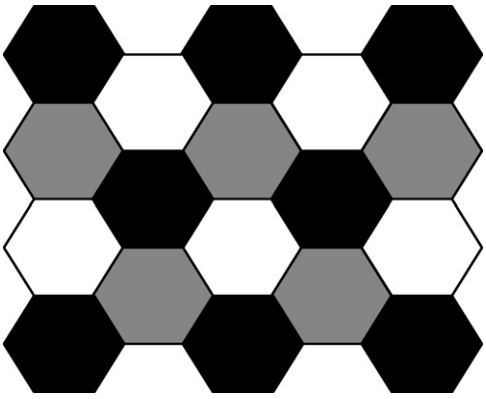

Fig. 1. Three-phase ideal microstructure with no similar grains touching in two dimensions. Each shade (black, gray, and white) represents a grain with a different chemical composition.

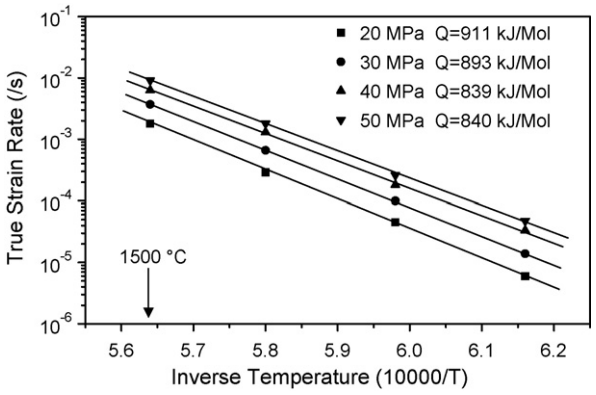

Fig. 3. Strain rate of three-phase alumina–mullite–TZP as a function of temperature plotted as an Arrhenius graph, with calculated activation energies. At 1500 °C, the strain rates can reach 10^{-2} s^{-1}.

which has few grains in contact with the same phase. The illustration in Fig. 1 shows that in two dimensions there could theoretically be no similar phase grain boundaries. This would limit grain growth, but also precludes easy diffusional accommodation of grain boundary sliding if each of the three phases has a different chemical composition. In three dimensions, grains are polyhedra that require four different phases in order to have no similar grain contacts. The challenge of designing such systems is to find four phases, which will be stable and not react during fabrication and high temperature deformation.

On a practical level, the three-phase system in oxide ceramics has provided excellent results in producing a stable grain size and high strain rates. Work by Kim et al.[5] showed that three-phase alumina–spinel–TZP could attain strain rates close to 1/s at 1650 °C. Work by Chen and Mecartney[6] has proved that the three-phase principle can be used with other ceramics compositions to generate high strain rates. Fig. 2 shows the microstructure of a three-phase 40 vol.% alumina, 30 vol.% mullite and 30 vol.% TZP material and Fig. 3 illustrates that high strain rates on the order of 10^{-2} s^{-1} can be achieved at moderate temperatures of 1500 °C.

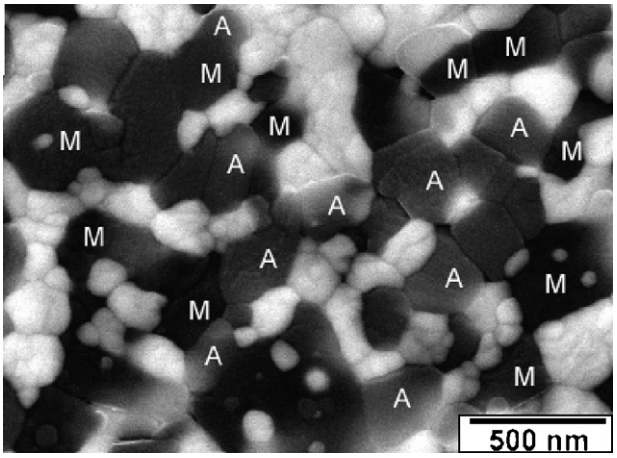

Fig. 2. Three-phase alumina (A), mullite (M) and zirconia (white grains) composite. Scanning electron microscopy in the backscattered mode with energy dispersive spectroscopy used to identify the composition of individual grains.

An unusual feature of this material, however, was the observation of dislocation generation primarily in the mullite-phase (Fig. 4). Dislocations appeared to be generated at stress concentrators at grain junctions due to the irregular shape of the mullite grains (mullite formed during processing by the reaction of colloidal silica and crystalline alumina). The dislocations traversed the grain, and most likely were absorbed by the opposite grain boundary sink. This behavior of dislocation assisted superplastic deformation in ceramic composites parallels that observed in superplastic metals.[9]

One challenge with these observations is that dislocation assisted plastic deformation in mullite is not well documented in the literature. One of the few reports of dislocations observed in polycrystalline mullite is by Hynes and Doremus[10] who reported that crept samples had a somewhat higher dislocation density

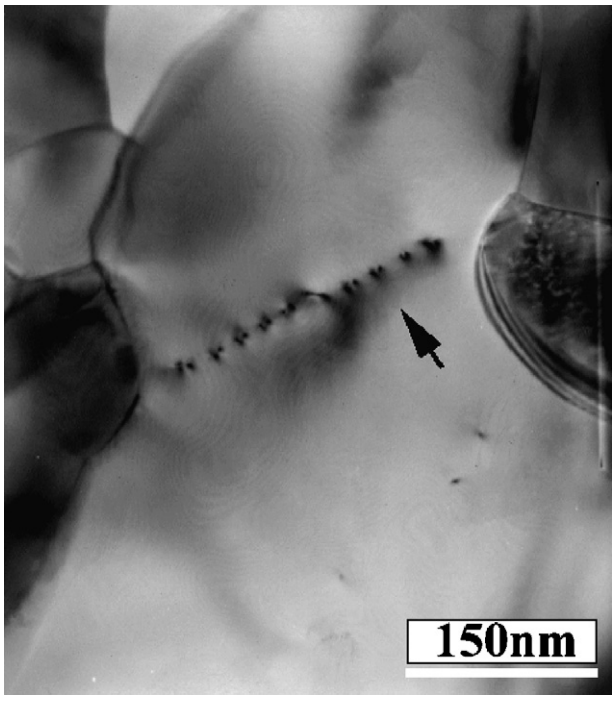

Fig. 4. Dislocations generated in mullite during deformation traversing the grain in this transmission electron microscopy image.

than uncrept samples, but their material contained a high volume fraction of glass which assisted the deformation. Low dislocation densities were also reported in SiC particle reinforced mullite deformed at high temperatures.[11] Indentation studies at room temperature on single crystal mullite found an amorphous region generated under the highest load of the indenter with dislocations observed at the end of the cracks generated.[12] Dislocation loops formed during single crystal growth of mullite were observed to have the Burgers vector parallel to the [0 0 1] direction.[13]

Considering all of the research on mullite, aptly summarized in a recent book edited by Schneider and Komarneni,[14] it may come as a surprise to learn that the slip system and Burgers vector for dislocations in mullite have not been conclusively determined. Indeed, there is only one published experiment by Pask's group on the high temperature deformation of single crystal mullite.[15] Researchers in this group attempted to compress mullite single crystals oriented 3° and 6° off the *c*-axis. The crystals subjected to stresses of up to 900 MPa at 1500 °C did not show plastic deformation. It was concluded that dislocations were not mobile under the testing conditions applied, presumably due to the complex crystal structure.[15] Their work has been cited by many researchers over the years to document that the excellent creep resistance of mullite is due to lack of dislocation slip.

However, if a compression axis is aligned perpendicular to the normal of the slip plane or perpendicular to the slip direction in single crystal experiments, there is no critical resolved shear stress to assist dislocation movement. The relationship between an applied stress (σ_a) and the resultant shear stress (τ) in a slip plane is a function of the angle between the normal to the slip plane and the deformation axis (ϕ) and the angle between the slip direction and the deformation axis (λ):

$$\tau = \sigma_a \cos\phi \cos\lambda \quad (2)$$

Consider the case of dislocations formed during single crystal growth, reported to have a [0 0 1] Burgers vector.[13] This Burgers vector would be consistent with the closest packed direction (shortest repeat direction) in the mullite unit cell. With a [0 0 1] Burgers vector, the slip plane normal would be perpendicular to [0 0 1], resulting in a zero Schmidt factor, and thus no slip is possible for single crystals deformed along [0 0 1]. The original single crystal experiments[15] could have been so closely aligned to [0 0 1] that the resolved shear stress was far below that required for slip, resulting in fracture instead.

The research reported in this paper is designed to better understand dislocation-assisted deformation in the mullite-phase. Single-phase mullite was used as a model system, as the grain size in three-phase alumina–mullite–TZP material is so small that the tilting experiments needed to characterize the dislocation character are difficult. In addition, energy dispersive spectroscopy in the transmission electron microscope is required to confirm that specific grains are mullite. The use of single-phase mullite offers the possibility of a larger grain size and a homogeneous composition making it easier to study dislocation generation during high temperature deformation.

2. Experimental procedure

Ceramic powders of 40 nm crystallite size alumina (Baikowski Inter. Corp., Charlotte, NC) and 15 nm diameter amorphous colloidal silica (Nissan Chemical Industries Ltd., Tokyo, Japan) were mixed in an attritor mill in isopropanol with the ratio of alumina to silica of 3:2 or 2:1. These compositions span the range of stoichiometry that mullite typically exhibits, from the polycrystalline form to single crystals. The powder mixtures were dried, sieved, and then cold isostatically pressed under 380 MPa. Small cylindrical deformation samples of 4 mm height and 2 mm diameter were prepared and sintered at 1450 °C for 1 h, a temperature known to produce mullite easily in three-phase mixtures. Bulk density of the samples was measured using the Archimedes method. Crystalline phase formed in the sintered samples were identified by X-ray diffraction (XRD) equipped with Cu Kα radiation. Samples were deformed in compression in a commercial ATS machine under constant load at 1450 °C, and the load remained on the sample during cooling to room temperature. Samples were examined by scanning electron microscopy (Zeiss Ultra 55 CDS) after polishing and thermal etching at 1450 °C for 30 min. Grain sizes were calculated using Olympus Microsuite™-M3 image analysis software that traces the shape of the grains and calculates the grain area, equivalent circle diameter, and perimeter. The equivalent circle diameters of the data from the grain analysis were multiplied by 1.74 to approximate the 3D grain size. Transmission electron microscopy (Philips CM20) using a double tilt stage was conducted after cutting, polishing, dimpling, and ion milling (Gatan DuoMill). Both SEM and TEM samples had to be coated with a conductive thin platinum or carbon layer to prevent charging in the microscopes.

3. Results and discussion

Mullite samples of 3:2 composition ($3Al_2O_3{\cdot}2SiO_2$) were 97% dense after sintering. Fig. 5(A) shows the jigsaw puzzle type of microstructure resulting from the reaction of amorphous colloidal silica and alumina. Powder X-ray diffraction indicated that a significant amount of cristobalite had formed in the mullite matrix, with a small trace of unreacted alumina also. Fig. 5(B) shows the microstructure of the 2:1 composition ($2Al_2O_3{\cdot}1SiO_2$). This material was only 94% dense initially. Powder X-ray diffraction showed a small amount of cristobalite in the mullite matrix, but greater amounts of unreacted alumina than in the 3:2 sample.

The deformation behavior under a compressive stress of 40 MPa at 1450 °C is shown in Fig. 6 for both of the compositions. The behavior is quite similar, although the strain rate is approximately twice as fast for the 3:2 sample compared to the 2:1 sample ($7 \times 10^{-6}\ s^{-1}$ compared to $3 \times 10^{-6}\ s^{-1}$ after 20,000 s of deformation). These strain rates are similar to those reported for mullite compositions tested at a similar temperature.[16] The 3:2 material had the greatest amount of unreacted silica, and the 2:1 sample had the highest amount of unreacted alumina, which would provide greater creep resistance for the latter.[17] The continual lowering of the strain rate with time indicates grain growth during deformation.

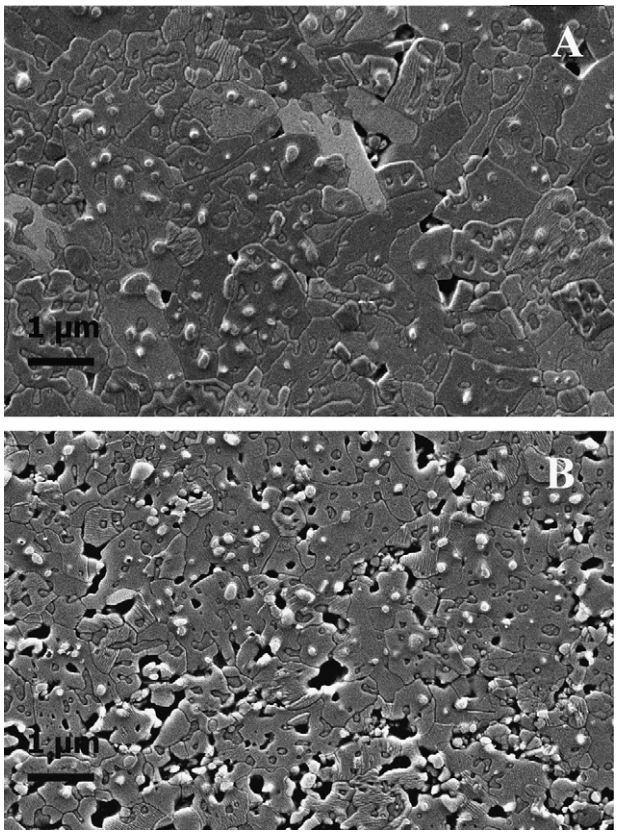

Fig. 5. Mullite prepared with (A) $3Al_2O_3$ and $2SiO_2$, and with (B) $2Al_2O_3$ and $1SiO_2$.

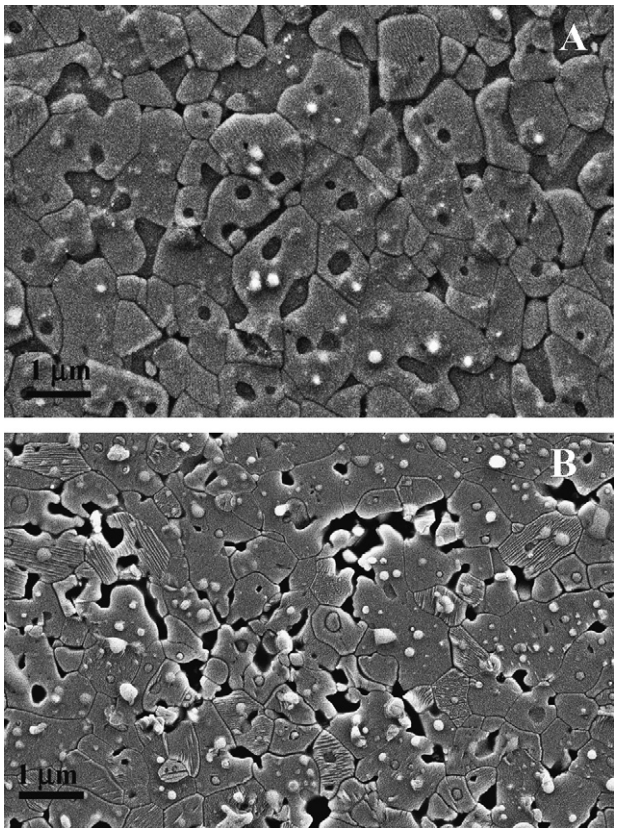

Fig. 7. Microstructure after deformation for mullite with (A) starting composition 3:2 and (B) starting composition 2:1. Note extensive cavitation in the high alumina sample (B) (compare to Fig. 5(A) and (B), prior to deformation).

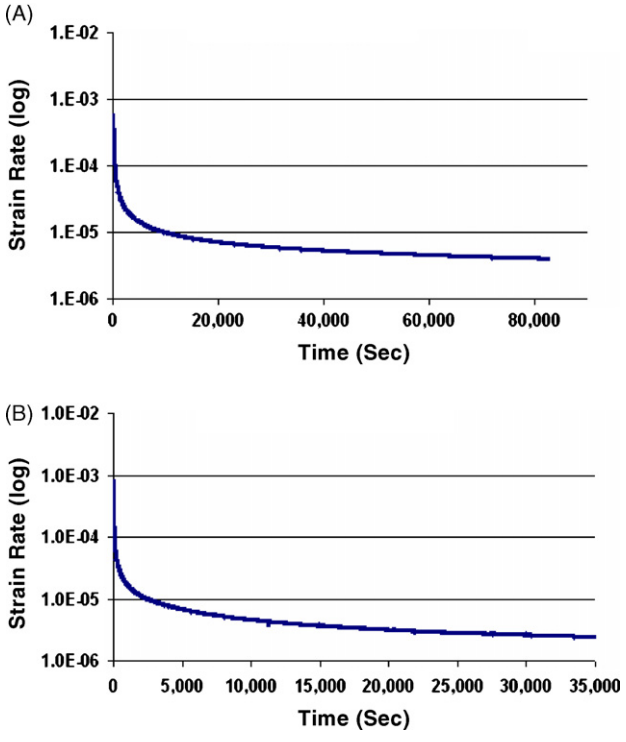

Fig. 6. Deformation under 40 MPa at 1450 °C for (A) 3:2 starting composition mullite and (B) 2:1 starting composition mullite.

Samples examined after deformation show a change to a more uniform grain shape as compared to the original samples. (compare Figs. 5 and 7.) The 3:2 samples maintained approximately the same density, 97%, but the 2:1 samples had a lower density after deformation, 91%, than initially. Significant cavitation can be seen in the 2:1 sample after deformation even though this sample was deformed only to 12% strain, compared to 35% deformation of the 3:2 sample. It is assumed that a small amount of a viscous phase from the excess amorphous silica assisted in deformation in the silica rich 3:2 composition, compared to the alumina rich 2:1 composition. This concurs with prior research, which found that silica rich mullites deform more easily at high temperatures than high alumina mullites.[18]

The grain size of the original samples is compared to the grain size of the deformed samples in Fig. 8. The data show different ways of calculating the grain size, using the average grain area, the equivalent circle diameter, and the perimeter. In all cases, grain growth during deformation is apparent, with an increase in equivalent circle diameter from 1.1 to 1.2 μm in the 3:2 samples and 0.8 to 1.1 μm in the 2:1 material. In addition, a change from a more tortuous grain shape to a more uniform grain shape is observed for 3:2 samples. If a uniform grain shape, such as a hexagon, dominates, then the perimeter would increase with an increase in grain diameter or grain area. The dramatic change in grain shape for 3:2 samples, resulting in a much more uniform grain shape after deformation, is the

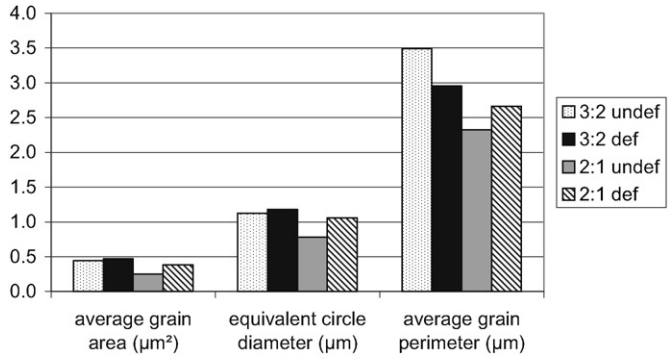

Fig. 8. Grain size data before and after deformation for 3:2 and 2:1 mullite samples.

reason for the decreased average grain perimeter after deformation (from 3.5 to 3.0 μm) even though the average grain size has increased.

Transmission electron microscopy studies were conducted on the mullite samples before and after deformation. Both 3:2 and 2:1 materials prior to deformation had some dislocations present in the grains often associated with the spherical alumina or cristobalite inclusions. After deformation there was a significant increase in the density of dislocations for both types of samples. However, dislocation tangles were rarely observed, most likely due to recovery due to climb. Both 3:2 and 2:1 materials were nominally the same $3Al_2O_3{\cdot}2SiO_2$ mullite composition (matching well with the powder diffraction file), with varying amounts of unreacted excess silica or excess alumina. The TEM data reported is primarily from 3:2 samples as the lower amount of porosity in these samples made sample preparation of large amounts of thin area easier.

In order to characterize the Burgers vector (**b**) of a dislocation, one can use the reciprocal lattice vector (**g**) of the planes that diffract electrons under a two-beam condition (meaning that one set of planes satisfies Bragg's Law). Under this condition, if $\mathbf{b}\cdot\mathbf{g}=1$, then the dislocation should be visible. If $\mathbf{b}\cdot\mathbf{g}=2$, then a double image of the dislocation can appear. When $\mathbf{b}\cdot\mathbf{g}=0$

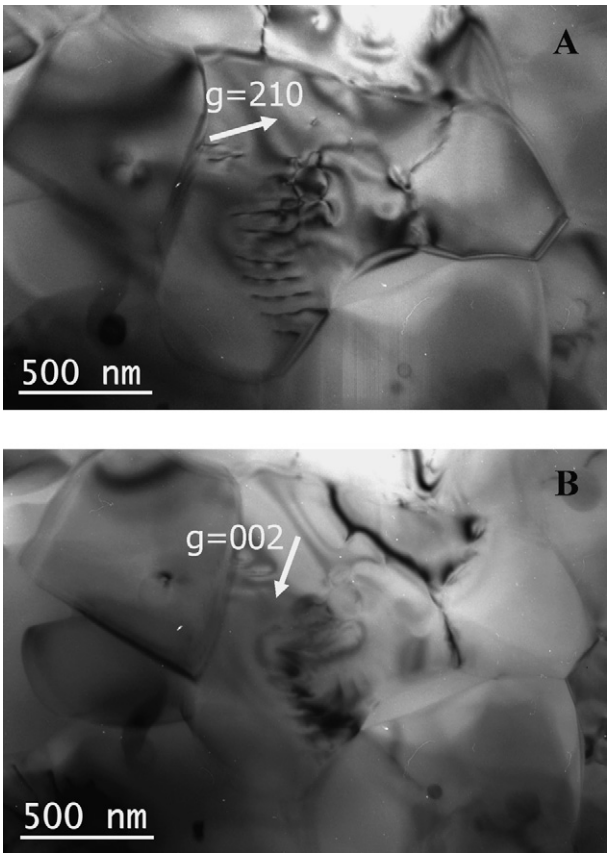

Fig. 9. Imaging dislocations in deformed 3:2 mullite. (A) (2 1 0) planes diffracting and dislocations visible, and (b) (0 0 2) planes diffracting and dislocations invisible. This particular set of dislocations cannot have **b** = [0 0 1].

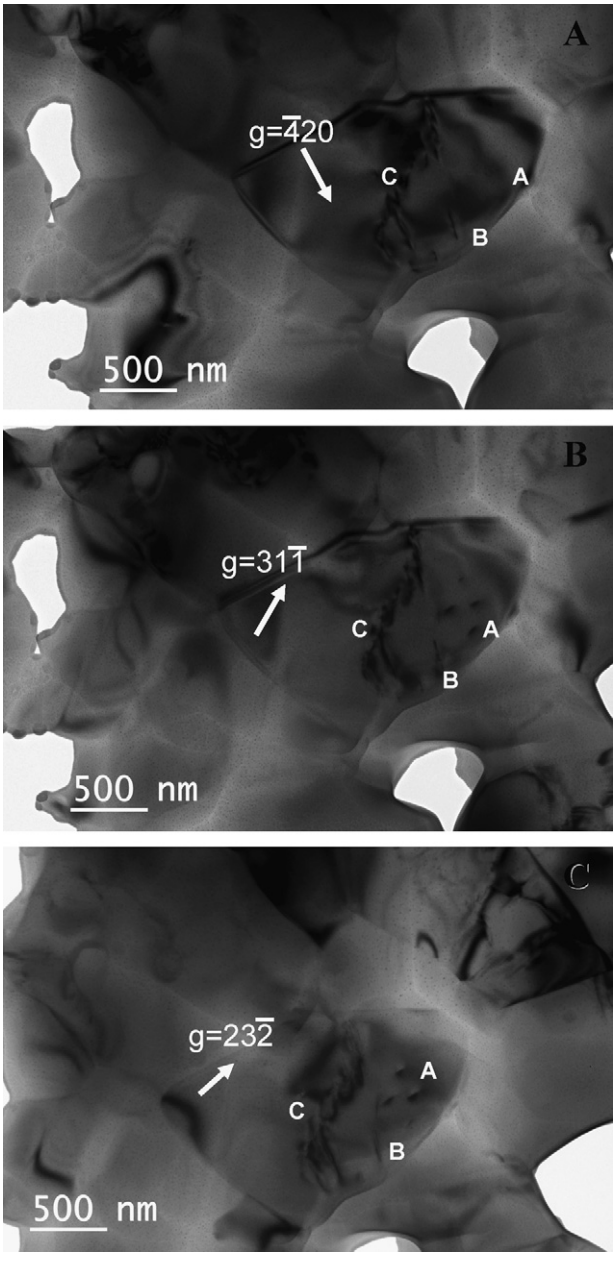

Fig. 10. Mullite grain with three groups of dislocations (white letters A, B, and C). Imaged using (A) [−4, 2, 0], (B) [3, 1, −1], and (C) [2, 3, −2]. Note that dislocations A disappear with **g** = [−4, 2, 0], indicating that this set may have **b** = [0 0 1], while dislocations B and C must be another type of Burgers vector.

for an edge dislocation, or $\mathbf{b} \cdot \mathbf{g} \times \mathbf{u} = 0$ for a screw dislocation (where $\mathbf{u}$ is the line direction), then the dislocation is not visible because the Burgers vector (the distortion) lies in the diffraction planes.

The TEM micrographs in Figs. 9 and 10 illustrate various diffracting conditions. If the dislocation character is $\mathbf{b} = [0\,0\,1]$, then the dislocation should be invisible (or weakly diffracting if a screw dislocation) under diffracting conditions of $[h\,k\,0]$. However it can be seen in Fig. 9 that under diffraction conditions of $\mathbf{g} = [2\,1\,0]$ dislocations are clearly visible, yet are invisible for $\mathbf{g} = [0\,0\,2]$, suggesting that the dislocation character may be of the type $\mathbf{b} = [h\,k\,0]$, but could not be $[0\,0\,1]$.

Three groups of dislocations are imaged in Fig. 10. Dislocations in groups B and C are visible under diffraction conditions of $\mathbf{g} = [\bar{4}\,2\,0]$, but dislocations in group A are invisible. For diffraction conditions $[3\,1\,\bar{1}]$ and $[2\,3\,\bar{2}]$, dislocations in group A are visible. This type of imaging would be possible if the dislocations in A were of the type $[0\,0\,1]$. Dislocations in group B are very weak under the diffraction conditions of $[2, 3, -2]$, and a Burgers vector of $[1\,0\,1]$ would be extinct under these conditions for dislocations in group B.

Although at this time it is not possible to definitively define the Burgers vector for dislocations in mullite, it appears that possibly three dislocation types are present. Dislocations of the type $\mathbf{b} = [0\,0\,1]$ may represent dislocations that nucleate during growth, as these are the type of dislocations which have been observed in 2:1 mullite single crystals grown from the melt.[13] These dislocations could be sessile and not glissile. A second set of dislocations, which match a different Burgers vector have been observed with $\mathbf{b}$ possibly $[1\,0\,1]$ and a third set of dislocations appear to match a Burgers vector of $[h\,k\,0]$. The second and third type of dislocations may be dislocations generated during deformation. Further work using compressive deformation of single crystal mullite cut with the appropriate orientation is proposed to conclusively determine the Burgers vector and slip plane for mullite, as has been done for other ceramic systems.[19]

4. Conclusions

Three-phase composites of alumina–mullite–TZP demonstrate a superplastic-like flow and a high strain rate superplasticity under compression, with evidence of dislocation accommodated grain boundary sliding. TEM studies of nominally single-phase mullite find that dislocations can easily be generated in mullite during deformation at 1450 °C under an applied stresses of 40 MPa. The dislocation character in polycrystalline mullite is not consistent with $\mathbf{b} = [0\,0\,1]$ for all dislocations, although some dislocations fit that characterization. Work is in progress to more fully characterize the dislocation character and slip system for mullite, which will require single crystal experiments.

Acknowledgements

Funds for this research were provided by NSF DMR grant 0207197 and by the UC LEADS program and the UC Irvine Henry Samueli School of Engineering Fellowship for undergraduate research. Dr. Hartmut Schneider is acknowledged for his encouragement and catalytic activity in nucleating new research collaborations by bringing together so many diverse scholars working in the field of mullite.

References

1. Wakai, F., Sakaguchi, S. and Matsuno, Y., Superplasticity of yttria-stabilized tetragonal ZrO_2 polycrystals. *Adv. Ceram. Mater.*, 1986, **1**, 259–263.
2. Kajihara, K., Yoshizawa, Y. and Sakuma, T., Enhancement of superplastic flow in tetragonal zirconia polycrystals with SiO_2 doping. *Acta Metall. Mater.*, 1995, **43**, 1235–1242.
3. Yoon, C. K. and Chen, I. W., Superplastic flow of two-phase ceramics containing rigid inclusions: zirconia mullite composites. *J. Am. Ceram. Soc.*, 1990, **73**, 1555–1565.
4. Dillon, R. P., Sosa, S. S. and Mecartney, M. L., Achieving tensile superplasticity in 8 mol% Y_2O_3 cubic stabilized ZrO_2 through the addition of intergranular silica. *Scripta Mater.*, 2004, **50**, 1441–1444.
5. Kim, B.-N., Hiraga, K., Morita, K. and Sakka, Y., A high-strain-rate superplastic ceramic. *Nature*, 2001, **413**, 288–291.
6. Chen, T. and Mecartney, M. L., A high-strain-rate alumina-based ceramic composite. *J. Am. Ceram. Soc.*, 2005, **88**, 1004–1006.
7. Xue, L. A. and Chen, I. W., Development of superplastic structural ceramics. *J. Am. Ceram. Soc.*, 1990, **73**, 2585–2609.
8. Cannon, W. R. and Langdon, T. G., Review: creep of ceramics. *J. Mater. Sci.*, 1983, **18**, 1–50.
9. Chen, T., Mohamed, F. A. and Mecartney, M. L., Threshold stress superplastic behavior and dislocation activity in a three-phase alumina–zirconia–mullite composite. *Acta Mater.*, 2006, **54**, 4415–4426.
10. Hynes, A. P. and Doremus, R. H., High temperature compressive creep of polycrystalline mullite. *J. Am. Ceram. Soc.*, 1991, **74**, 2469–2475.
11. Gustafsson, S., Falk, L. K. L., Pitchford, J. E., Clegg, W. J., Liden, E. and Carlstrom, E., Development of microstructure during creep of mullite and mullite 5 vol% SiC nanocomposite. *Key Eng. Mater.*, 2001, **206–213**, 1145–1148.
12. Schmücker, M., Schnieder, H. and Kriven, W. M., Indentation induced amorphization in mullite single crystals. *J. Am. Ceram. Soc.*, 2003, **86**, 1821–1822.
13. Stacy, W. T. and Guse, W., X-ray topographic study of Czochralski grown mullite. *J. Crystal Growth*, 1976, **35**, 153–158.
14. Schneider, H. and Komarneni, S., ed., *Mullite*. Wiley VCH, Weinheim, Germany, 2005.
15. Dokko, P. C., Pask, J. A. and Mazdiyasni, K. S., High temperature mechanical properties of mullite under compression. *J. Am. Ceram. Soc.*, 1977, **60**, 150–155.
16. Okada, K. and Schneider, H., Mechanical properties of mullite ceramics. In *Mullite*, ed. H. Schneider and S. Komarneni. Wiley VCH, Weinheim, Germany, 2005, p. 320.
17. Okamoto, Y., Fukudome, H., Hayashi, K. and Nishikawa, T., Creep deformation of polycrystalline mullite. *J. Eur. Ceram. Soc.*, 1990, **6**, 161–168.
18. Torrecillas, R., Calderon, J. M., Moya, J. S., Reece, M. J., Davies, C. K. L., Olagnon, C. and Fantozzi, G., Suitability of mullite for high temperatures applications. *J. Eur. Ceram. Soc.*, 1999, **19**, 2519–2527.
19. Mecartney, M. L., Donlon, W. T. and Heuer, A. H., Plastic deformation in CaO stabilized ZrO_2 (CSZ). *J. Mater. Sci.*, 1990, **15**, 1063–1065.